UTILIZATION OF NEAR REAL-TIME NOAA-AVHRR SATELLITE OUTPUT FOR EL NIÑO INDUCED DROUGHT ANALYSIS IN INDONESIA (CASE STUDY: EL NIÑO 2015 INDUCED DROUGHT IN SOUTH SULAWESI)

Amsari Mudzakir Setiawan[1,2], Yonny Koesmaryono[2], Akhmad Faqih[2,*)] and Dodo Gunawan[1]
[1]Center for Climate Change Information, The Indonesia Agency for Meteorology, Climatology and Geophysics (BMKG)
[2]Applied Climatology, Graduate School of Bogor Agricultural University (IPB)
[*)]e-mail: akhmadfa@apps.ipb.ac.id; amsari.setiawan@bmkg.go.id
Received: 10 June 2016; Revised: 5 July 2016; Approved: 31 August 2016

Abstract. Drought is becoming one of the most important issues for government and policy makers. National food security highly concerned, especially when drought occurred in food production center areas. Climate variability, especially in South Sulawesi as one of the primary national rice production centers is influenced by global climate phenomena such as El Niño Southern Oscillation or ENSO. This phenomenon can lead to drought occurrences. Monitoring of drought potential occurrences in near real-time manner becomes a primary key element to anticipate the drought impact. This study was conducted to determine potential occurrences and the evolution of drought that occurred as a result of the 2015 El Niño event using the Vegetation Health Index (VHI) from the National Oceanic and Atmospheric Administration (NOAA) Advanced Very High Resolution Radiometer (AVHRR) satellite products. Composites analysis was performed using weekly Smoothed and Normalized Difference Vegetation Index (or smoothed NDVI) (SMN), Smoothed Brightness Temperature Index (SMT), Vegetation Condition Index (VCI), Temperature Condition Index (TCI), and Vegetation Health Index (VHI). This data were obtained from The Center for Satellite Applications and Research (STAR) - Global Vegetation Health Products (NOAA) website during 35-year period (1981-2015). Lowest potential drought occurrences (highest VHI and VCI value) caused by 2015 El Niño is showed by composite analysis result. Strong El Niño induced drought over the study area indicated by decreasing VHI value started at week 21st. Spatial characteristic differences in drought occurrences observed, especially on the west coast and east coast of South Sulawesi during strong El Niño. Weekly evolution of potential drought due to the El Niño impact in 2015 indicated by lower VHI values (VHI < 40) concentrated on the east coast of South Sulawesi, and then spread to another region along with the El Nino stage.

Keywords: *drought, near real-time monitoring, NOAA-AVHRR, VHI, VCI, TCI, El Niño*

1 INTRODUCTION

Weather and climate are important issues and give significant impact to policies taken by the government, especially regarding to the national food security. Global and regional climate conditions can potentially trigger a drought in Indonesia (Setiawan 2014), resulting reduction in national rice production (Surmaini *et al.*, 2015). Climate variability in Indonesia is strongly influenced by the global climate phenomenon such as El Niño Southern Oscillation or ENSO (Ropelewski and Halpert 1987; Chang *et al.*, 2004; Qian et al. 2010). Warm phase of ENSO, known as El Niño, generally affect decreases rainfall and lead to drought in most parts of

Indonesia (Harger 1995; D'Arrigo and Wilson 2008; Erasmi et al. 2009; Setiawan 2011; Setiawan 2014).

The climatic condition in South Sulawesi as one of the national rice production center also influenced by drought due to El Niño events. This impact generally shown by ratio between the area of rice production area damaged by drought and the total cropping area, represented by Paddy Drought Impact Index (PDII), especially during August to October period (Surmaini et al. 2015). South Sulawesi is also listed as a region prone to drought. Recorded 108 drought events occurred during 30-years period (1979 – 2009) (BNPB 2010).

Different climatological rainfall characteristics between western and eastern region of South Sulawesi (Setiawan 2007) suspected to be causes treatment for potential drought occurrences impact can't be done using similar way. Recognition about teleconection pattern between Sea Surface Temperature (SST) against the drought is needed to complete the drought monitoring information so that it can be used to make drought prediction (Sivakumar *et al.*, 2014). The influences of ENSO (represented by SST anomaly over Niño 3.4 region) on the rainfall in South Sulawesi are more significant than the influence of Indian Ocean Dipole (IOD) (Hidayat *et al.*, 2016). Therefore, the potential for drought monitoring in near real-time becomes a key element in efforts to anticipate drought impacts induced.

Operational near real-time global drought monitoring and identification has done by utilizing National Oceanic and Atmospheric Administration (NOAA) Advanced Very High Resolution Radiometer (AVHRR) satellite. Outcomes NOAA-AVHRR from Smoothed and Normalized Difference Vegetation Index (NDVI or smoothed) (SMN) is commonly used as a substitute for rainfall data in quantifying drought (Jiang et al. 2008; Jalili *et al.*, 2014). Vegetation health index (VHI), vegetation condition index (VCI) and temperature condition index (TCI) are other drought indices that can be used for drought quantification using satellite technology. VHI has been widely used throughout the world (Zargar *et al.,* 2011; Kogan *et al.*, 2013) to quantify the agricultural drought, such as the United States (Kogan et al. 2012; Anderson et al. 2013), Rusia (Kogan *et al.*, 2015), Iran (Jalili *et al.*, 2014), India (Bhuiyan *et al.*, 2006), Bangladesh (Nizamuddin *et al.*, 2015), China (Zhang *et al.*, 2016) and West Java Indonesia (Sholihah *et al.*, 2016). The objectives of this study was to carry out the drought potential and evolution in South Sulawesi during strong El Niño event in 2015 using VHI, VCI and TCI from NOAA-AVHRR Near Real-Time outcomes.

2 MATERIALS AND METHODOLOGY

The study was conducted using outcome from National Oceanic and Atmospheric Administration (NOAA) Advanced Very High Resolution Radiometer (AVHRR) satellite products (Wei Guo 2013) such as Smoothed and Normalized Difference Vegetation Index (or smoothed NDVI) (SMN) and Smoothed Brightness Temperature Index (SMT). SMN is an output-based index of satellites that can be used to estimate the level of greenness of the vegetation with the value of +1 to -1. If SMN value is low (0.1 or less), showing can be interpreted that surface of the earth is rock or sand. Intermediate values (0.2 to 0.5) can be interpreted as an agricultural area that has been harvested, and the high value (0.6 to 0.9) are interpreted as forest or crops area in the peak stage of growth. SMT can explain thermal condition of the plant, where which the higher the SMT interpreted as drier vegetation condition (Kogan, 1990).

Potential drought occurrences also can be quantified using another calculation outcome from NOAA – AVHRR, such as Vegetation Condition Index (VCI) and Temperature Condition Index (TCI). Vegetation Condition Index (VCI) is an anomalous value of the Normalized Difference Vegetation Index (NDVI), which can be used to estimate the humidity condition. The higher VCI value associated with higher humidity can be detected from the vegetation. Less than 40 VCI value indicates humidity stress occured, while the ideal condition is indicated by more than 60 VCI value (Kogan 1995; Kogan 1997). VCI value for weeks or months to j is calculated from (Kogan 1995; Kogan 1997):

$$VCI_j = \frac{NDVI_j - NDVI_{min}}{NDVI_{max} - NDVI_{min}} x100 \qquad (2\text{-}1)$$

with $NDVI_{max}$ and $NDVI_{min}$ represented maximum and minimum NDVI value for current week or month and $NDVI_j$ is NDVI value for week or month.

TCI can be used to estimate the thermal conditions of vegetation. Less than 40 TCI value of indicates the vegetation is under pressure (stress) thermally, while the condition conducive to the plant indicated by the value of more than 60. TCI value obtained by relatively similar to the VCI, but using the Brightness Temperature (BT) input for following, maximum and minimum week or month (Kogan 1995; Kogan 1997).

Vegetation health index (VHI), VHI value is representation of vegetation conditions obtained by combining moisture and temperature conditions, so it have better effectiveness in representing agricultural drought (Kogan 1995; Zargar *et al.*, 2011; Kerdprasop and Kerdprasop 2016). The calculation of this value is obtained from the Vegetation Condition Index (VCI) and Temperature Condition Index (TCI) (Kogan 1995; Kogan 1997) by the equation:

$$VHI = aVCI + (1 - a)TCI \qquad (2\text{-}2)$$

with a is a weighting factor for VCI and TCI. VHI value is used to indicate the level of health of vegetation greenness level. Higher VHI value indicates greener vegetation. Less than 35 VHI value of indicates the start of the medium drought, and less than 15 can be associated with severe drought s have occured (Kerdprasop and Kerdprasop 2016).

Time series analysis has been done using the calculation results of various indices (SMN, SMT, VCI, TCI and VHI) to capture general climatological properties over study area. These indices are freely available and can be accessed through The Center for Satellite Applications and Research (STAR) - Global Vegetation Health Products website (www.star.nesdis.noaa.gov/smcd/emb/VCI/VH/index.php) in a weekly time scale during relatively long period (1981-2015).

Sea surface temperature (SST) anomalies data in the tropical Pacific Ocean Niño 3.4 region (5° N-5° S, 120° W-170° W) generally used as a reference for determining whether ENSO are in warm condition (El Niño) or condition cold (La Niña). The moving average for 3-month s is a standard method that is done to the intensity of ENSO. During 1981 to 2015 period, at least three times stronger El Niño events recorded: 1982/1983, 1997/1998 and 2015/2016 (Chen *et al.*, 2016; Jan Null 2016).

Composite analysis was conducted to determine the comparison of the potential drought occurrence and its evolution during strong El Niño compared to normal conditions (weekly average value for 35-years period), indicated by each drought indices. Formula used to composite calculation relatively similar with an average formula, except for selected time period are used:

$$[\bar{X}]_w = \frac{1}{n}\sum_{i=1}^{n}[X_i]_w \qquad (2\text{-}3)$$

$[\bar{X}]_w$ = is a composite value of each index used for week w, n is the number of periods in the data, $[\bar{X}_i]_w$ = is the index data in year i, i = 1,2,3, ..., n, and w = week = 1, 2, 3, ..., 52. In this case, n = 3 as representation of El Niño year (year 1 = 1982, year 2 = 1997 and year 3 = 2015).

3 RESULTS AND DISCUSSION

Data for each drought index as outcomes from NOAA-AVHRR satellite analyzed to determine the variability of the whole series of data and the weekly evolution of potential drought due to El the El Niño 2015 event in South Sulawesi. Drought evolution, then compared with other strong El Niño event in the previous year, namely 1997 and 1982 as well as climatological conditions of the all average year 1981-2015 and composite analysis was performed for all strong El Niño events during the study period. Time series comparison of SMN and SMT over South Sulawesi can be seen from Figure 3-1.

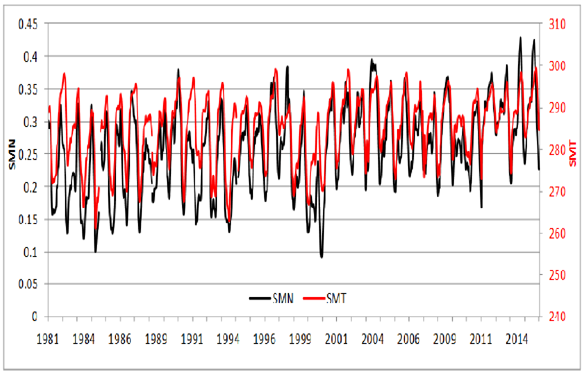

Figure 3-1: Time series of grid averaged SMN (black line) and SMT(red line) value over South Sulawesi for 35-year period

Interannual variability of SMN and SMT can be recognized from the time series plot. SMN and SMT generally have the same relative phase (Figure 3-1). Seasonal variations can be seen from the comparison climatological average value plotting (Figure 3-2). Both SMN and SMT increase started at week 9 and begin to decrease starting at week 35 for SMN and week 41 for SMT.

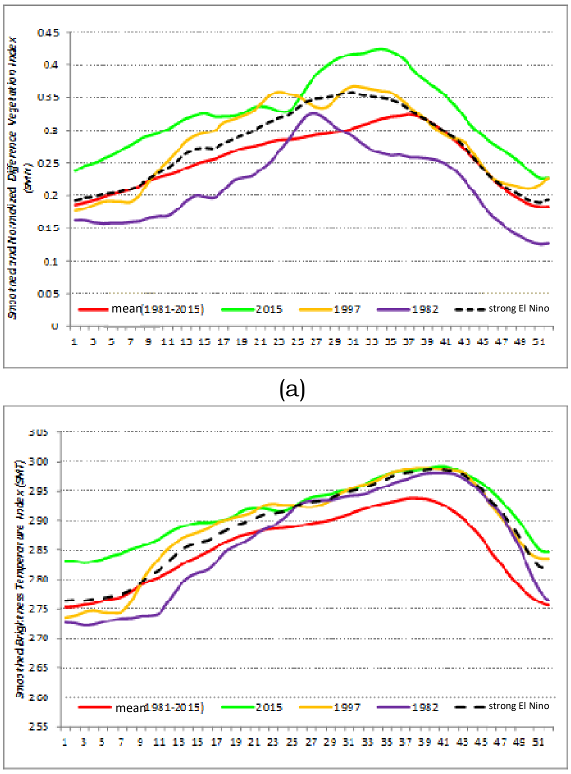

(b)

Figure 3-2: Comparison of weekly SMN (a) and SMT (b) values during El Niño events in 2015 (green), 1997 (yellow), and 1982 (purple). Weekly composites of three strong El Niño years (dashed black line) against climatological average from 1981 to 2015 (red).

El Niño conditions generally impact on the relatively higher than the average SMN value, except for the El Niño 1982 event. Meanwhile, from the SMT perspective, El Niño generally impact on the increased value SMT above the average start from week 9 for 1997 events and week 21 for 1982 events. The SMT value for the 2015 event higher than the average throughout the year.

Further analysis conducted using other drought parameter derived from NOAA – AVHRR satellite product. VCI and TCI as input for VHI calculation was analyzed during strong El Niño period to get better understanding of the drought respond over the study area. Interannual variability of VCI and TCI are generally identified from the entire series plot for all time study period. VCI and TCI generally have the opposite phase (Figure 3-3).

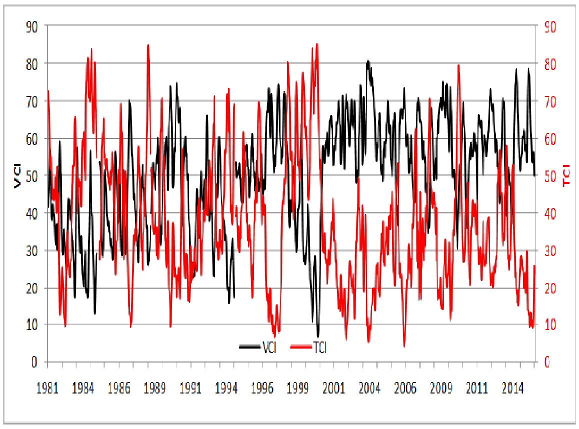

Figure 3-3: Time series of monthly grid averaged VCI (black line) and TCI (red line) values over South Sulawesi for 35-year period

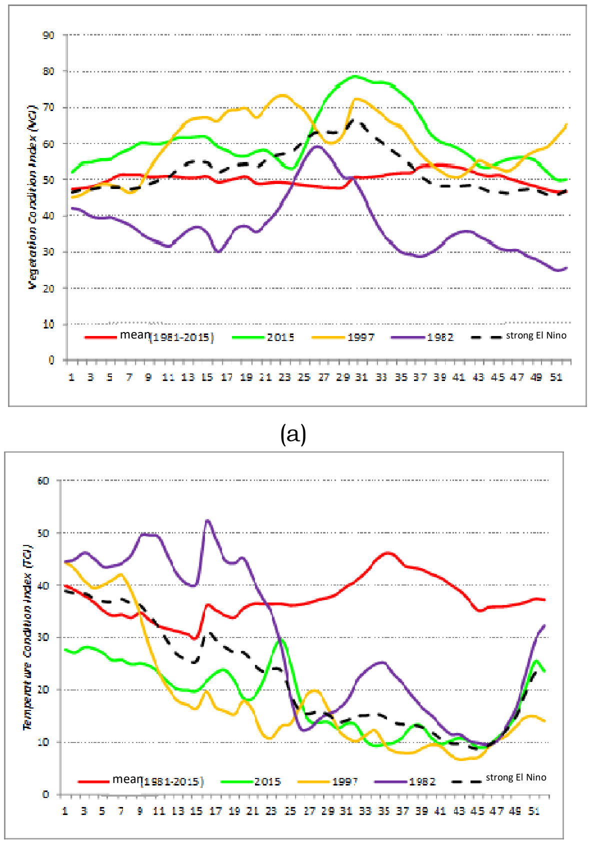

(a)

(b)

Figure 3-4: Comparison of weekly VCI (a) and TCI (b) values during El Niño in 2015 (green), 1997 (yellow), 1982 (purple). Weekly composites of three strong El Niño years (dashed black line) against climatological average from 1981 to 2015 (red).

It is reasonable to consider the physical properties of moisture (represented by VCI) and temperature (represented by TCI) have opposite characteristic nature. Seasonal variations of humidity and temperature in this region are difficult to identify from the average climatological plotting results because in the tropical region this parameter generally has relatively uniform values during all year. El Niño conditions generally impact on the ralatively higher than the average VCI value, except for the El Niño in 1982 occurrence. Meanwhile, based on TCI perspective, El Niño generally start to decrease the TCI value until below their average at week 9 for 1997 and week 21 for the 1982 event. However, during the 2015 event, lower than the average SMT value recorded throughout the year (Figure 3-4).

VHI value which is a combination of VCI and TCI value in strong El Niño is generally lower than the climatological average since week 21 for 1997 and most all-overs the year for 2015 and 1982 (Figure 3-5). This VHI values condition generally caused by the decreased value of TCI during these El Niño periods.

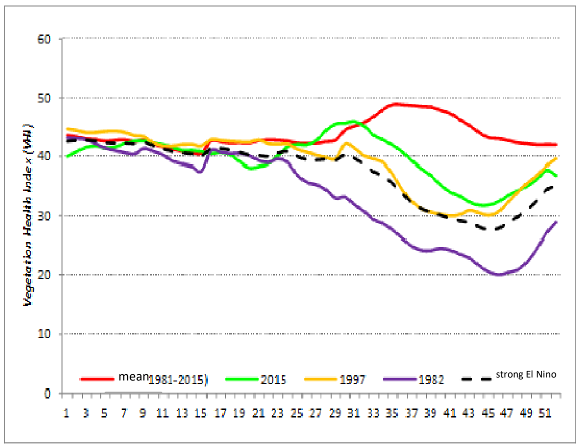

Figure 3-5: Comparison of grid average weekly Vegetation Health Index (VHI) values in South Sulawesi during El Niño events in 2015 (green), 1997 (yellow) and 1982 (purple). A composite three-year strong El Niño (dashed black line) against 35-years climatological average (1981-2015) (red).

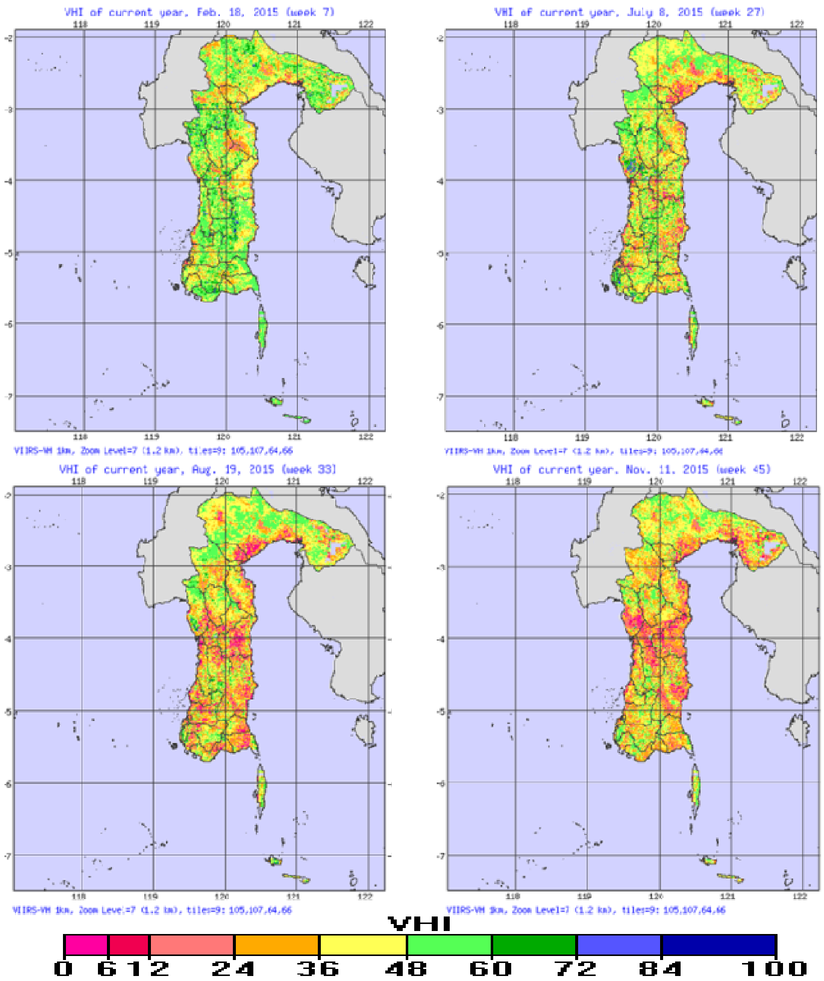

Figure 3-6: Spatial evolution pattern of VHI values in 2015 during El Niño occurred (top left), onset (top right), growing period (bottom left) and mature stage of El Niño (bottom right) (Source: star.nesdis.noaa. gov)

Spatial analysis conducted on VHI in 2015 result shows that there are spatially distinctive characteristics of drought between west coast and the east coast South Sulawesi (Figure 3-6). Evolution of low VHI value (VHI<40) spatial distribution associated with drought occurrence during early stage of El Niño February 2015 generally is concentrated in the eastern coast of South Sulawesia and the west coast of South Sulawesi is still in relatively favorable conditions (dominated by high VHI value). West coast of South Sulawesi experienced the rainy season during this month (Setiawan 2007). Lower VHI value distribution began to spread same times as of the El Niño onset, growing El Niño phase and reached its peak. Generally, the most affected region by El Niño in 2015 from the VHI point of view are located on the east coast of South Sulawesi.

4 CONCLUSION

Composites analysis results showed that potential drought caused by 2015 El Niño is relatively low compared to 1997/ 1998 and 1982/1983. The Strong El Niño impact of drought over the study area generally indicated by decreasing VHI value started at week 21st. Weekly evolution of potential drought due to the El Niño impact in 2015, indicated by lower VHI values (VHI<40), starts seeing on the east coast of South Sulawesi in week 21 and then spread to another region during the next stage of the El Niño phase. There are spatially typical characteristic differences in drought occurrences between west coast and east coast of South Sulawesi during strong El Niño.

ACKNOWLEDGEMENTS

The first author thank to the Indonesia Agency for Meteorology Climatology and Geophysics (BMKG) for providing a scholarship for his PhD program and NOAA STAR Satellite Products and data dissemination for providing the data used in this research.

REFERENCES

Anderson MC, Hain C., Otkin J., Zhan X., Mo K., Svoboda M., Wardlow B., Pimstein A., (2013), An Intercomparison of Drought Indicators Based on Thermal Remote Sensing and NLDAS-2 Simulations with U.S. Drought Monitor Classifications. J Hydrometeorol 14:1035–1056. doi: 10. 1175/JHM-D-12-0140.1.

Bhuiyan C., Singh RP, Kogan FN, (2006), Monitoring drought dynamics in the Avavalli region (India) using different indices based on ground and remote sensing data. Int J Appl Earth Obs Geoinformatics 8:289–302.

BNPB NA for DM, (2010), Peta kejadian bencana kekeringan di Indonesia tahun 1979 - 2009. In: 22 Sept. 2010. http:// geospasial.bnpb.go.id/2010/09/23/peta-kejadian-bencana-kekeringan-di-indonesia-tahun-1979-2009/Accessed 19 Jun 2016.

Chang CP, Wang Z, Ju J, Li T,, (2004), On the relationship between western maritime continent monsoon rainfall and ENSO during northern winter. J Clim 17:665–672. doi: 10.1175/1520-0442(2004)017 <0665:OTRBWM>2.0.CO;2.

Chen S., Wu R., Chen W., (2016), Genesis of westerly wind bursts over the equatorial western Pacific during the onset of the strong 2015 – 2016 El Niño. doi: 10.1002/asl.669.

D'Arrigo R., Wilson R., (2008), El Nino and Indian Ocean influences on Indonesian drought: implications for forecasting rainfall and crop productivity. Int J Climatol 28:611–616.

Erasmi S., Propastin P., Kappas M., Panferov O., (2009), Spatial Patterns of NDVI Variation over Indonesia and Their Relationship to ENSO Warm Events during the Period 1982–2006. J Clim 22:6612–6623. doi: 10. 1175/2009 JCLI2460.1.

Harger JRE, (1995), Air-temperature variations and ENSO effects in Indonesia, the Philippines and El Salvador: ENSO patterns and changes from 1866-1993. Atmos Environ 29:1919–1942. doi: 10. 1016/1352-2310(95)00017-S.

Hidayat R., Ando K., Masumoto Y., Luo JJ, (2016), Interannual Variability of Rainfall over Indonesia: Impacts of ENSO and IOD and Their Predictability. IOP Conf Ser Earth Environ Sci 31:12043. doi: 10.1088/ 1755-1315/31/1/012043.

Jalili M., Gharibshah J., Ghavami SM, Beheshtifar M., Farshi R., (2014), Nationwide prediction of drought conditions in Iran based on remote sensing data. IEEE Trans Comput 63:90–101. doi: 10.1109/TC.2013.118.

Jan Null C., (2016), El Niño and La Niña Years and Intensities. http://ggweather.com/ enso/oni.htm. Accessed 1 May 2016.

Jiang L., Tarpley JD, Mitchell KE, et al., (2008), Adjusting for long-term anomalous trends in NOAA'S global vegetation index data sets. IEEE Trans Geosci Remote Sens 46:409–421. doi: 10.1109/TGRS.2007. 902844.

Kerdprasop K., Kerdprasop N., (2016), Rainfall Estimation Models Induced from Ground Station and Satellite Data. In: Proceedings of the International MultiConference of Engineers and Computer Scientists. IMECS 2016, Hongkong,

Kogan F., Adamenko T., Guo W., (2013), Global and regional drought dynamics in the climate warming era. Remote Sens Lett 4:364–372. doi: 10.1080/2150704X. 2012. 736033.

Kogan F., Guo W., Strashnaia A., Kleshenko A., Chub O., Virchenko O., (2015), Modelling and prediction of crop losses from NOAA polar-orbiting operational satellites. Geomatics, Nat Hazards Risk 7:886–900. doi: 10.1080/19475705.2015.1009178.

Kogan F., Salazar L., Roytman L., (2012), Forecasting crop production using satellite-based vegetation health indices in Kansas, USA. Int J Remote Sens 33:2798–2814. doi: 10.1080/01431161.2011.621464.

Kogan FN, (1995), Application of vegetation index and brightness temperature for drought detection. Adv Sp Res 15:91–100. doi: 10.1016/0273-1177(95)00079-T.

Kogan FN, (1997), Global Drought Watch from Space. Bull Am Meteorol Soc 78:621–636. doi: 10.1175/1520-0477(1997) 078<0621: GDWFS>2.0.CO;2.

Nizamuddin M., Akhand K., Roytman L., Kogan F., Goldberg M., (2015), Using NOAA/ AVHRR based remote sensing data and PCR method for estimation of Aus rice yield in Bangladesh. 9488:1–10. doi: 10.1117/12.2086186.

Qian J-H, Robertson AW, Moron V., (2010), Interactions among ENSO, the Monsoon, and Diurnal Cycle in Rainfall Variability over Java, Indonesia. J Atmos Sci 67:3509–3524. doi: 10.1175/2010JA S3348.1.

Ropelewski CF, Halpert MS, (1987), Global and Regional Scale Precipitation Patterns Associated with the El Niño/Southern Oscillation. Mon Weather Rev 115:1606–1626. doi: 10.1175/1520-0493(1987) 115 <1606:GARSPP>2.0.CO;2.

Setiawan AM, (2014), Drought Characteristics in Indonesia Related to Warm ENSO Episodes. APEC Climate Center, Busan.

Setiawan AM, (2011), Determination of Reference ENSO Index for Indonesian Region Based on Correlation Analysis of Spatial and Temporal Pattern with Standardized Precipitation Index (SPI). Institut Teknologi Bandung (ITB).

Setiawan AM, (2007), Mapping of South Sulawesi Rainfall Distribution using Arcview GIS [in Indonesian]. Makassar State University (UNM).

Sholihah RI, Trisasongko BH, Shiddiq D., (2016), Identification of Agricultural Drought Extent Based on Vegetation Health Indices of Landsat Data: Case of Subang and Karawang, Indonesia. Procedia Environ Sci 33:14–20. doi: 10.1016/j.proenv. 2016. 03. 051.

Sivakumar MVK, Stefanski R., Bazza M., et al., (2014), High Level Meeting on National Drought Policy: Summary and Major Outcomes. Weather Clim Extrem 3:126–132. doi: 10.1016/j.wace.2014.03.007.

Surmaini E., Hadi TW, Subagyono K., Puspito NT, (2015), Early detection of drought impact on rice paddies in Indonesia by means of Niño 3.4 index. Theor Appl Climatol 121:669–684. doi: 10.1007/ s00704-014-1258-0.

Wei Guo, (2013), AVHRR Vegetation Health Product (AVHRR-VHP) User Guide.

Zargar A., Sadiq R., Naser B., Khan FI, (2011). A review of drought indices. Environ Rev 19:333–349. doi: 10.1139/a11-013.